Strain-Free Polarization Superlattice in Silicon Carbide: A Theoretical Investigation

Peter Deák,[1] Adam Buruzs,[2] Adam Gali,[2] and Thomas Frauenheim[1]

[1]*Theoretical Physics, University of Paderborn, Warburger Strasse 100, Paderborn D-33098, Germany*

[2]*Department of Atomic Physics, Budapest University of Technology and Economics, Budafoki út 8, Budapest H-1111, Hungary*

(Received 6 August 2005; published 13 June 2006)

A strain-free superlattice of inversion domains along the hexagonal axis of SiC is investigated by theoretical calculations. The induced polarization causes a zigzag shape in the band edges, leading to spatial separation of photoexcited carriers and to an effective band gap narrowing tunable over a wide range by the geometry and on a smaller scale by the intensity of the excitation. Calculations on the SiC surface indicate that preparation of such a superlattice might be possible in atomic layer epitaxy with properly chosen sources and temperatures.

DOI: 10.1103/PhysRevLett.96.236803 PACS numbers: 73.21.Cd, 73.43.Cd, 78.67.Pt

In 1970, Esaki and Tsu suggested two ways for the one-dimensional (1D) periodic modulation of the potential in semiconductor single crystals: variation of the composition or of the impurity density [1]. The former causes quasi-2D quantum confinement due to the band offset, and such *heterostructure superlattices* quickly became the basis for modern optoelectronic devices. The latter, a periodic variation of *n*- and *p*-doped layers (possibly separated by intrinsic regions), gives rise to an electric field with a sawtooth-shaped potential, which provides for carrier confinement with spatial separation of electrons and holes. These *n-i-p-i superlattices* show a tunable absorption edge with strong optical nonlinearity, as well as giant ambipolar carrier diffusion [2]. In this Letter, we point out the possibility for a superlattice without varying either the composition or the impurity distribution. A third possibility, a *polytype superlattice* based on band offsets, has already been proposed and later synthesized in the binary compound semiconductor SiC [3]. Here we describe the properties and feasibility of a *polarization superlattice* in SiC, with an intrinsic electric field variation similar to that of *n-i-p-i* superlattices. Our superlattice consists of inversion domains along the [0001] axis of one given hexagonal polytype of SiC. In the neighboring inversion domains, the sequence of the atoms—and with that the polarization of the domain—is reversed, leading to a superlattice of $[(\mathrm{SiC})_n(\mathrm{CSi})_m]$ units. Our calculations in 4*H*-SiC show that the zigzag-shaped variation of the electrostatic potential makes the tuning of the effective band gap possible over a range of $\sim$1 eV without loss in the absorption coefficient. The band gap lowering is more than what can be achieved in GaAs *n-i-p-i* structures, can be sustained up to higher excitation densities, and is insensitive to carrier scattering. While such a polarization superlattice is unlikely in III-V or II-VI compounds, we will show that atomic layer epitaxy (ALE) of SiC offers a good chance for synthesis.

The (0001) inversion domain boundaries (IDBs) in our system consist of ''wrong'' (Si-Si or C-C) bonds. IDBs of various orientation frequently occur in polycrystalline SiC and also during heteroepitaxial growth [4]. IDBs can be polar or nonpolar, containing only one or both types of wrong bonds, respectively. Theoretical studies of III-V/II-VI superlattices have shown that, due to compensation between close lying donor and acceptor bonds, nonpolar IDBs are the more stable ones (and often even a reconstruction occurs to annihilate the wrong bonds), while abrupt polar interfaces are usually unstable [5]. In SiC, the octet sum of valences remains even in case of wrong bonds, and the mismatch between the Si-Si and C-C bond lengths causes substantial strain in nonpolar IDBs. In contrast, no stress whatsoever is involved with the polar IDBs in our superlattice, where the length of the wrong bonds can be adjusted by a uniform translation of the grains along the [0001] axis. Our calculated formation energy for a pair of (0001) polar IDBs in 4*H*-SiC is only 3.1 $\mathrm{J/m^2}$ (or 1.6 eV for a pair of wrong bonds), lower than that of a pair of nonpolar (110) IDBs in cubic SiC (3.6 $\mathrm{J/m^2}$ [6]). It should be noted that the extreme case $[(\mathrm{SiC})_\infty(\mathrm{CSi})_1]$ corresponds to a planar array of antisite pairs in bulk SiC. Antisite pairs are high energy defects, but it has been shown that aggregation into an infinite (0001) planar array reduces their energy by 80%, making the pairs in the array the lowest energy defects in SiC by far [7]. Reconstruction of individual antisite pairs requires considerable activation energy [8], and, once formed, the metastable inversion domains could be reinverted at an even higher energy cost.

We have considered polarization supercells in 4*H*-SiC with periods $L = 4c$, $6c$, and $8c$, where $c = 10.05$ Å is the length of the 4*H* unit cell (4 Si-C double layers) along the hexagonal axis. The bond lengths, Mulliken charges, and total energies are essentially the same in the three cases, and the calculated bands show no dispersion parallel to the c axis. In the $L = 6c$ case, we also studied the effect of varying the distance between the IDBs within the period. Unless otherwise noted, the results shown here are for IDBs at hexagonal sites, $d = L/2$ apart. The total energy has been minimized with respect to the atomic positions in the framework of density functional theory. To avoid the gap problem associated with standard implementations, like the local density approximation (LDA), we applied a semiempirical one-parameter ($\lambda = 0.2$) hybrid functional

[9], mixing LDA [10] with Hartree-Fock exchange. This choice of the mixing parameter results in band gaps of 2.42, 3.09 and 3.33 eV for 3*C*-, 6*H*-, and 4*H*-SiC, respectively, in very good agreement with experiment, while it somewhat overestimates the band gap of silicon (1.44 eV) and underestimates that of diamond (5.12 eV). The calculated (experimental) lattice constant, cohesive energy, and bulk modulus for 3*C*-SiC are 4.39 (4.36) Å, 7.14 (6.34) eV, and 2.20 (2.24) GPa, respectively. All geometry optimization and electronic structure calculations have been carried out with the hybrid functional. As a test, we have also performed pure LDA calculations with *GW* corrections for the electronic structure of the smallest supercell as described in Ref. [11]. The energy of the highest occupied and the lowest unoccupied interface states with respect to the perfect valence and conduction band edges in the LDA, *GW*, and hybrid calculations were $+0.98$, $+1.07$, $+1.05$ eV and -0.32, -0.31, -0.28 eV, respectively. On the one hand, the agreement between the *GW* and hybrid results (both giving the correct band gap) justifies our use of the hybrid functional. On the other hand, the agreement in the relative positions with LDA shows that the localized states shift with the band edges. Therefore, the imaginary part of the dielectric function, $\varepsilon_2(\omega)$, was calculated in LDA, using the random phase approximation without local field correction and many body effects, as described in Ref. [11]. The result has then been shifted up by the difference between the experimental and LDA-calculated indirect gap of bulk 4*H*-SiC. For the hybrid functional calculations, the CRYSTAL code was used with a 21* valence basis set [12], while the LDA and *GW* calculations were carried out with the VASP package using plane waves (up to a cutoff of 31 Ry), and the projector augmentation wave method [13]. A $8 \times 8 \times 2$ *k*-point set in the Brillouin zone (BZ) of the supercell was applied in the ground state hybrid calculations. In the case of the dielectric function, Blöchl's linear tetrahedron method [14] was used for the BZ summation, with altogether 9408 *k* points in the bulk primitive BZ and 3456 in the BZ of the smallest supercell which is reduced 4 times relative to the primitive one [15].

In hexagonal polytypes of SiC, the double layers are inequivalent, giving rise to spontaneous polarization [16]. In 4*H*-SiC, we calculate a transfer of $\Delta q = 0.02e$ Mulliken charge between silicon sites with cubic and hexagonal environments. In the inversion domain superlattice, there is an additional rearrangement of the charge distribution, with a net transfer of $\Delta Q = 0.22e$ Mulliken charge from the C-C double layer to the Si-Si one [17], which diminishes the repulsion between the identically charged atoms. (Even so, the repulsion between carbon atoms—strongly felt over the short distance—makes the C-C bond longer than usual, 1.62 Å, while the Si-Si bond length is 2.34 Å.) As a consequence, the change in the average electrostatic potential [18] shows a zigzag shape and is negative for electrons at the C-C and positive at the Si-Si layer. In the three structures with $d = L/2$, the amplitude of the zigzag shows a linear dependency on d, with $\Delta V_{\max}/d = 0.013\,\mathrm{eV/Å}$. Triangular wells in the electrostatic potential can lead to electron and hole confinement to the region of the C-C and the Si-Si IDBs, respectively. Indeed, we see 2D minibands in the band structure and some gap states, in addition. A C-C and a Si-Si related occupied state appear at 1.3 and 0.5 eV above the local valence band (VB) edge, respectively. These are analogous to the highest occupied e_g orbital of ethane and a_{1g} orbital in disilane. A C-C related unoccupied orbital, just below the local conduction band (CB) edge, is analogous to the first unoccupied a_{2u} orbital of ethane. Occupied states related to Si-Si bonds in SiC are known to appear in the gap [19], but here the elongated C-C bonds introduce a bonding-antibonding pair as well. These interface states are more localized than those found at nonpolar IDBs [6,20] and comparable to the quantum well states in ternary monolayer superlattices (see, e.g., [21]). The C-C related states are localized within $\sim$8 a.u. (0.43 nm), while the Si-Si related ones within $\sim$11 a.u. (0.58 nm) of the respective double layers. Such interface states can be interpreted qualitatively in terms of a simple bulk band edge model [22,23], as arising from the potential well represented by the Si-Si and C-C double layers. Using the method of Ref. [24], these wells can be determined from the position of the gap states with respect to the local band edges and from the localization of the wave functions, as shown in Fig. 1.

Periodically varying electrical fields occur also in heterostructure superlattices [25]: (i) when the two interfaces within one period are not identical, as, e.g., in an isovalent III-V quaternary superlattice, (ii) when "donor bonds" between anions and "acceptor bonds" between cations appear at the opposite interfaces, as, e.g., in nonisovalent ternary superlattices, or (iii) when a macroscopic polarization field exists in one or both superlattice regions, like in ternary order-disorder superlattices or in polytype superlattices. The two interfaces are not identical in our case either, but the field is not the same in the two halves of the superlattice, as should be in case (i). The alternating sign is similar to that of case (ii) or the *n-i-p-i* superlattice, but here we have no donors and acceptors between which compensation could occur. The field arises not due to the inherent polarization (charge transfer $\Delta q = 0.02e$) as in case (iii) but is the result of an induced polarization ($\Delta Q = 0.22e$) in the inversion domains. (Note that with IDBs at cubic sites the inherent polarization would even be opposite to the induced one.) In a first approximation, the potential due to the charge transfer ΔQ between the two IDBs can be written in atomic units as $\Delta V = 4\pi\Delta Q z_i/\varepsilon_r A$, where ε_r is the relative dielectric constant of SiC and A is the unit cell surface area. In the supercell, we have two capacitors with $z_1 = d$ and $z_2 = L - d$. Because of the periodic boundary condition, the maximum amplitude of the potential is $\Delta V_{\max} = 4\pi\Delta Q(L - d)d/2L\varepsilon_r A$. For $L = 2d$, this is in line with the linear d dependence of $\Delta V_{\max}/d$ observed in the calculations, so the constant part can be replaced by the value obtained

there:

$$\frac{\Delta V_{\max}}{d} = 2\frac{L-d}{L} \cdot 0.013 \text{ eV/Å}. \quad (1)$$

This formula reproduces the results of the self-consistent calculations for $L \neq 2d$ as well. The picture emerging from Fig. 1 is analogous to that of δ-doped n-i-p-i superlattices [26] and has also similar consequences. The effective band gap between holes at a "peak" of the VB and electrons at a neighboring "valley" of the CB will be smaller than the gap of the perfect crystal [by twice the value given in Eq. (1)]. Figure 2 shows $\varepsilon_2(\omega)$ for the smallest supercell ($L = 4c$), parallel to the c axis. As expected from Eq. (1), the onset of absorption is about 0.5 eV lower than in the perfect lattice. It rises also more steeply in the region immediately above the indirect band gap than in the perfect lattice. The calculated absorption coefficient at 4.5 eV (see inset in Fig. 2) is $\sim 5 \times 10^5$ cm^{-1}, 25 times higher than in the perfect lattice. In addition, a very strong absorption appears in the 5.0–5.5 eV region, independent of L. This is due to strong direct transitions between the (e_g, a_{1g})- and a_{2u}-type states which are strongly localized to the IDBs and have similar (near parallel) energy dispersion.

According to Eq. (1), the effective gap can be tuned by two independent parameters L and d. For a constant d/L ratio, it diminishes with increasing L, while lowering d/L simultaneously ensures that the overlap between neighboring VB peak and CB valley states does not diminish. Keeping $d = 2c$, as in Fig. 2, the effective gap can be diminished by about 1 eV without any loss in the absorption coefficient. The maximal range for tuning the gap is about 2.5 eV (until the unoccupied state on the C-C IDB does not fall below the occupied one over Si-Si). This can be reached with $d_{\min} = 5c$ at $L = 115c$, resulting in an estimated loss of about 1 order of magnitude in the absorption coefficient. Therefore, the tuning range is about twice as large as in the case of a GaAs n-i-p-i superlattice. The separation of optically excited carriers will partially compensate the built in polarization field and increase the effective band gap. This effect would cause the variation of the absorption coefficient with excitation intensity, leading to nonlinear optical behavior. Taking the Mulliken charge as a guide, a concentration of electron-hole pairs up to $\sim 10^{21}$ cm^{-3} could be produced without fully compensating the polarization field, which is not influenced by carrier scattering, either.

The crucial question, of course, is whether a SiC polarization superlattice can be synthesized at all. Formation of metastable layer structures is often facilitated by the thermodynamics of the surface during deposition at steps [21] or via surface reconstruction [27]. It has already been demonstrated that monolayer-by-monolayer ALE growth of cubic SiC is possible in the 1000–1200 °C temperature range [28]. The condition for producing IDBs during [0001] growth is a self-limiting deposition of a "wrong atomic layer" (by applying a wrong cycle sequence). This is possible if: (i) a stable reconstruction exists with a Si double layer on the Si face and a C double layer on the C face, and (ii) if these layer sequences are not destroyed by the attack of C and Si atoms, respectively, in the following "normal" deposition cycle. Condition (i) is obviously met at the Si face, where, in the case of Si excess, the (3×3) reconstruction is stable below 950 °C and contains a Si double layer (with an additional 1/3 monolayer plus adatoms) [29]. To check on condition (ii), we have performed LDA calculations, similar to those in Ref. [29] but with an added C atom. The energetically most favorable absorption site between the pyramids of the Si adatoms is above the Si double layer as shown in Fig. 3(a). This configuration is 0.6 eV more stable than any position *between* the two Si

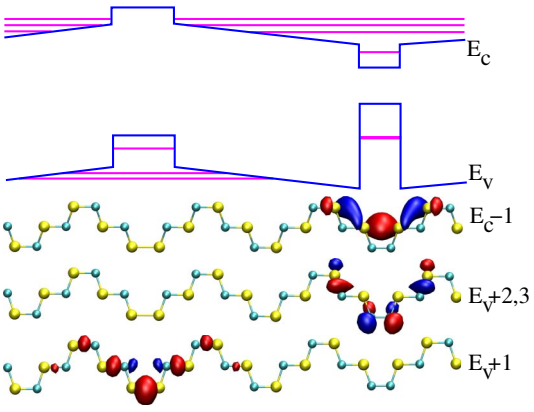

FIG. 1 (color online). Upper part: Confined states of free carriers in the polarization superlattice ($L = 4c$, $d = 2c$), depicted in a simple bulk band edge model. The localization of the gap states is shown in the lower part. The lobes show negative and positive isosurfaces along the chain of Si and C atoms (larger light and smaller dark spheres—yellow and blue in color—respectively).

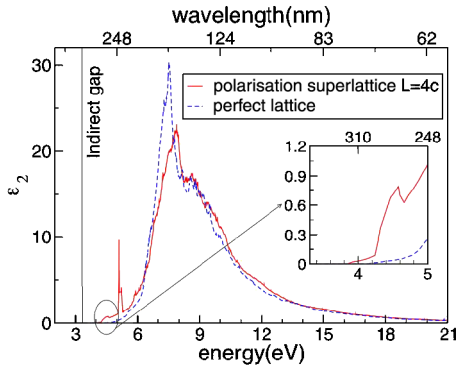

FIG. 2 (color online). Comparison of the imaginary part of the relative dielectric functions parallel to the c axis for the perfect lattice (dashed blue line) and the polarization superlattice with $L = 4c$ (solid red line). The inset shows a magnification of the onset of the spectra.

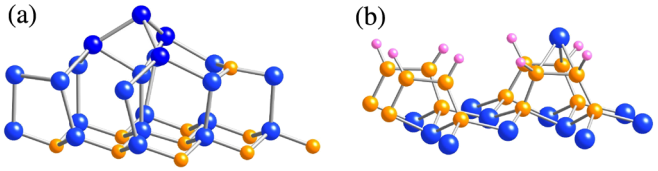

FIG. 3 (color online). (a) C atom adsorbed on the 3×3 reconstructed Si face and (b) Si atom absorbed on the C_2H_2 covered C face of a {0001} slab of hexagonal SiC. Large dark, medium, and small light spheres (blue, ochre, and pink in color) denote Si, C, and H atoms, respectively.

monolayers. Obviously, a considerable activation energy would also be needed to push the carbon atom through the upper Si layer. Therefore, if the temperature is kept low, the incoming C atoms will break the ''unnatural'' parallel-to-surface Si-Si bonds, restoring the topology of the substrate, rather than penetrate below the surface Si layer and break the vertical Si-Si bonds. The pyramids are similar to those on the high temperature $R3 \times R3$ reconstruction, where it has been shown [30] that the C atoms attack the side of the pyramids, resulting in the continuation of the proper element sequence. The C face with atomic carbon excess in ultrahigh vacuum becomes graphitic. However, our LDA calculations show that C_2H_2 easily adsorbs onto the $(000\bar{1})$ face of SiC, forming ethene bridges [see the left-hand side of Fig. 3(b)]. Monolayer coverage (one C atom per every surface carbon) can be achieved in a (2×1) or (2×2) pattern. Independent of its starting position with respect to such a surface, the conjugate gradient optimization places an additional Si atom into a position between and above two bridges, as shown on the right-hand side of Fig. 3(b). Three of the four bridging C atoms become tetravalent, and the Si adatom is above a Si site of the SiC lattice. Arrival of further Si atoms would lead to the restoration of the lattice topology. Based on these results, we see a good chance of preparing a polarization superlattice with proper temperature control and choice of precursors in an ALE process.

In summary, we have shown that the binary semiconductor SiC offers the possibility of a $[(SiC)_n(CSi)_m]$ inversion domain superlattice, different from the ones known so far (i.e., without variation in composition, doping, or polytype). The induced zigzag-shaped polarization potential causes a decrease in the energy of the absorption edge, which can be tuned with the parameters m and n over at least 1 eV. This structure would show nonlinear optical behavior up to high excitation densities, usable in Q switching in the low-wavelength range. The tunable band gap and the long lifetime of the spatially separated carriers could make it possible to fabricate very efficient on-chip solar cells for powering high frequency SiC devices.

We are indebted to J. Neugebauer and A. Zrenner for valuable advice. The support of the Hungarian OTKA Grant No. F-038357 and the German-Hungarian bilateral research fund No. 436 UNG113/137/0 (MTA -No. 118) is greatly appreciated.

[1] L. Esaki and R. Tsu, IBM J. Res. Dev. **14**, 61 (1970).
[2] K. H. Gulden *et al.*, Phys. Rev. Lett. **66**, 373 (1991).
[3] F. Bechstedt and P. Käckell, Phys. Rev. Lett. **75**, 2180 (1995); A. Fissel *et al.*, Appl. Surf. Sci. **184**, 37 (2001).
[4] K. Tanaka and M. Kohayama, J. Electron Microsc. **51**, 265S (2002); P. Pirouz, C. M. Chorey, and J. A. Powell, Appl. Phys. Lett. **50**, 221 (1987).
[5] W. R. L. Lambrecht, C. Amador, and B. Segall, Phys. Rev. Lett. **68**, 1363 (1992); J. E. Northrup, J. Neugebauer, and L. T. Romano, Phys. Rev. Lett. **77**, 103 (1996).
[6] W. R. L. Lambrecht and B. Segall, Phys. Rev. B **41**, 2948 (1990).
[7] E. Rauls, A. Gali, P. Deák, and Th. Frauenheim, Mater. Sci. Forum **433–436**, 491 (2003).
[8] E. Rauls, Z. Hajnal, A. Gali, P. Deák, and Th. Frauenheim, Mater. Sci. Forum **353–356**, 435 (2001).
[9] A. D. Becke, J. Chem. Phys. **104**, 1040 (1996).
[10] J. P. Perdew and A. Zunger, Phys. Rev. B **23**, 5048 (1981).
[11] J. Furthmüller, G. Cappellini, H.-Ch. Weissker, and F. Bechstedt, Phys. Rev. B **66**, 045110 (2002).
[12] V. R. Saunders *et al.*, *CRYSTAL2003 User's Manual* (University of Torino, Torino 2003).
[13] G. Kresse and J. Hafner, Phys. Rev. B **49**, 14 251 (1994); G. Kresse and J. Furthmüller, Phys. Rev. B **54**, 11 169 (1996).
[14] P. E. Blöchl, O. Jepsen, and O. K. Andersen, Phys. Rev. B **49**, 16 223 (1994).
[15] The convergence with the k set was tested.
[16] A. Qteish, V. Heine, and R. J. Needs, Phys. Rev. B **45**, 6534 (1992).
[17] Apart from the immediate neighbors of the IDBs, the charge on other atoms of the supercell essentially does not change with respect to the perfect lattice. The calculated charge transfer is similar to the one found for a superlattice of low-angle IDB-like grain boundaries [20].
[18] A. Baldereschi, S. Baroni, and R. Resta, Phys. Rev. Lett. **61**, 734 (1988).
[19] A. Gali *et al.*, Phys. Rev. B **67**, 155203 (2003); A. T. Blumenau, Phys. Rev. B **68**, 174108 (2003).
[20] P. Rulis, W. Y. Chung, and M. Kohyama, Acta Mater. **52**, 3009 (2004).
[21] M. Albrecht *et al.*, Phys. Rev. B **71**, 035314 (2005).
[22] M. J. Shaw, P. R. Briddon, and M. Jaros, Phys. Rev. B **52**, 16 341 (1995).
[23] H. Kroemer, C. Nguyen, and B. Brar, J. Vac. Sci. Technol. B **10**, 1769 (1992).
[24] H. Iwata, U. Lindefelt, S. Öberg, and P. R. Briddon, Phys. Rev. B **65**, 033203 (2002).
[25] S. Froyen, A. Zunger, and A. Mascarenhas, Appl. Phys. Lett. **68**, 2852 (1996).
[26] M. B. Johnston, M. Gai, G. Li, and C. Jagadish, J. Appl. Phys. **82**, 5748 (1997).
[27] S. Froyen and A. Zunger, Phys. Rev. Lett. **66**, 2132 (1991).
[28] T. Fuyuki, T. Yoshinobu, and H. Matsunami, Thin Solid Films **225**, 225 (1993).
[29] U. Starke *et al.*, Phys. Rev. Lett. **80**, 758 (1998).
[30] M. Righi *et al.*, Phys. Rev. Lett. **91**, 136101 (2003).